Published in final edited form as:
Respir Physiol Neurobiol. 2009 December 31; 169(3): 303–314. doi:10.1016/j.resp.2009.09.013.

Mutation in the myelin proteolipid protein gene alters BK and SK channel function in the caudal medulla

Catherine A. Mayer[1,*], **Wendy B. Macklin**[2], **Nanthawan Avishai**[3], **Kannan Balan**[1], **Christopher G. Wilson**[1], and **Martha J. Miller**[1]

[1]Department of Pediatrics, Case Western Reserve University, Cleveland, OH

[2]Department of Cell and Developmental Biology, University of Colorado Denver Health Sciences, Aurora, CO

[3]Lerner Research Institute, Cleveland Clinic, Cleveland, OH

Abstract

Proteolipid protein (*Plp*) gene mutation in rodents causes severe CNS dysmyelination, early death, and lethal hypoxic ventilatory depression (Miller et al. 2004). To determine if *Plp* mutation alters neuronal function critical for control of breathing, the nucleus tractus solitarii (nTS) of four rodent strains were studied: myelin deficient rats (MD), myelin synthesis deficient (Plp^{msd}), and Plp^{null} mice, as well as shiverer (Mbp^{shi}) mice, a myelin basic protein mutant. Current-voltage relationships were analyzed using whole-cell patch-clamp in 300μm brainstem slices. Voltage steps were applied, and inward and outward currents quantified. MD, Plp^{msd}, and Plp^{null}, but not Mbp^{shi} neurons exhibited reduced outward current in nTS at P21. Apamin blockade of SK calcium-dependent currents and iberiotoxin blockade of BK calcium-dependent currents in the P21 MD rat demonstrated reduced outward current due to dysfunction of these channels. These results provide evidence that *Plp* mutation specifically alters neuronal excitability through calcium-dependent potassium channels in nTS.

Keywords

myelin proteolipid protein; BK channel; SK channel; Plp^{null} mouse; Plp^{msd} mouse; Mbp^{shi} mouse; Pelizaeus-Merzbacher disease

1. Introduction

Myelin proteolipid protein (PLP) is the major protein in CNS myelin, accounting for 50% of myelin-associated proteins in the central nervous system. Mutations in the *Plp* gene, which are X-linked, have been found in rodents, such as the myelin deficient (MD) rat, and the myelin synthesis deficient mouse (Plp^{msd}). These mutations cause severe dysmyelination in the CNS, associated with oligodendrocyte death and non-myelinated or poorly myelinated axons, as well as abnormal axoglial junctions (Dentinger et al. 1982; Rosenbluth 1987).

[*]Corresponding author. Catherine A. Mayer, Department of Pediatrics, Case Western Reserve University, 11100 Euclid Ave., Cleveland, OH 44106 caa4@case.edu. .

Most rodents with mutations in the *Plp* gene develop tremors, ataxia, and seizures in the second week of life, and early death by postnatal day (p) 21–23. (Knapp 1996; Garbern et al. 1999; Yool et al. 2000). *Plp* mutations in humans are associated with a leukoencephalopathy, Pelizaeus-Merzbacher disease, which bears many pathophysiologic similarities to the rodents with *Plp* mutations (Boulloche and Aicardi 1986). The mechanisms by which mutations in the *Plp* gene cause a complex and potentially fatal leukoencephalopathy are incompletely understood.

Recently, we showed that rodents with mutations in the *Plp* gene exhibit an abnormal hypoxic response. The response to 8% oxygen is characterized by an initial increase in ventilation over 1–2 min, followed by severe ventilatory depression terminating in apnea (Miller et al., 2003, 2004). This abnormality in ventilatory response to hypoxia develops between P18 and P21, the age at which seizures begin and early death occurs. At this age, 72% of pups die with a single 5 minute exposure to 8% O_2, and 100% die after 2 exposures. These rodents exhibit normal minute ventilation during sleep, and no apnea was observed. The defect in breathing control in these rodents is limited to the hypoxic ventilatory response, for the hypercapnic response is normal (Miller et al. 2003, 2004). This finding suggests that the dysfunction in ventilatory response to hypoxia lies within the neuronal network which controls the response to hypoxia. This hypoxic response depends on chemosensory impulses which arise within the peripheral chemoreceptors, the carotid bodies (Prabhakar 2000). Sensory nerve fibers whose perikarya lie within the petrosal ganglion convey chemosensory impulses from the carotid body to brainstem neurons in the caudal commissural area of the nucleus tractus solitarius (nTS) and to a lesser extent to the ventrolateral medulla (Finley and Katz, 1992; Housley et al. 1987). Projections from the commissural nTS to the retrotrapezoid nucleus (RTN) provide a powerful stimulus to this critical area which integrates central and peripheral chemoreceptor input (Bodineau et al. 2000, Guyenet et al. 2008, Takakura et al. 2006). From this area the stimulus may be conveyed to the central pattern generator and to premotor neurons which drive phrenic motor output. Thus, response to chemoreception depends on integrity of function at several levels, including the first central synapse in the commissural subnucleus of the nTS.

Our own work as well as that of other groups has shown that PLP mRNA and protein are expressed in neurons in the caudal medulla of the rodent, including the nTS, during early postnatal development (Greenfield et al. 2006; Miller et al. 2009). The finding that the *Plp* gene is expressed in neurons is of potential pathophysiologic importance for two reasons; 1. *Plp* gene mutation can alter expression of other genes (Kumar et al. 1990), and 2. the form of PLP protein expressed in response to mutation is misfolded and may be toxic to cells due to the ER-stress response (Gow et al. 1994; Gow and Lazzarini 1996; Tosic et al. 1996, 1997).

Therefore, we explored the hypothesis that mutation in the *Plp* gene could produce dysfunction in the neurons within the commissural nTS, the subnucleus which receives afferent input from the peripheral chemoreceptors. We compared whole-cell patch-clamp recordings of nTS neurons in *in vitro* brainstem slices in normal rodents, and rodents with three different mutations in the *Plp* gene—the myelin deficient (MD) rat, the myelin synthesis deficient (Plp^{msd}) mouse, and the Plp^{null} mouse—to determine whether *Plp* gene mutation alters the electrophysiological properties of neurons in the nTS and whether these effects occur at the same age at which lethal hypoxic ventilatory depression develops. In addition, in order to determine if dysmyelination alone could cause alteration of the electrophysiologic properties of neurons in the medulla, we studied the shiverer mouse (Mbp^{shi}) which has dysmyelination due to a mutation in the myelin basic protein gene but no alteration in control of breathing (Miller et al. 2004).

2. Materials and Methods

Animals

The myelin deficient rat has a missense mutation on the X-linked *Plp* gene, which results in severe hypomyelination and early death (Simons and Riordan 1990). Male MD rat pups and male littermate controls (WT) were bred by mating Plp^{MD}+/− females with normal Wistar males. Affected males were detected by the onset of tremor at day 11–14 (Csiza and deLahunta, 1979). Rats were studied at one of two age groups, P12–14 (n=63) or P20–24 (n=95). Plp^{msd} mice, which have a missense mutation at a different amino acid in the *Plp* gene have a phenotype that is similar to the MD rat (Gencic and Hudson 1990). These mice were bred by mating Plp^{msd} +/− females with WT males. Affected males were identified by the presence of tremor and seizures at P18 (Meier and McPike 1969). Plp^{msd} mice were studied at P21 (n=8). Plp^{null} +/− females (Klugmann et al. 1997) and WT males were bred and male progeny were genotyped using PCR. The PLP transgenic null mouse has targeted inactivation of the translation start site for PLP and the splice product DM20, and no PLP or DM20 protein is synthesized (Klugman et al. 1997). This mouse has none of the major pathologic features of the MD rats or Plp^{msd} mice. Plp^{null} and WT littermates were studied at P21 (n=6 for each group). Mbp^{shi} mice, which exhibit a dysmyelinating phenotype due to a mutation in the myelin basic protein (*Mbp*) gene, were obtained from Charles River Laboratories (Wilmington, MA), and subsequently bred by mating Mbp^{shi} +/− males and females. Affected animals were identified by the presence of visible tremor at P21 (Readhead and Hood, 1990). Mbp^{shi} mice were studied at P21–25 (n=10). All protocols for breeding and physiological research met with previous approval from the Institutional Care and Use Committee of Case Western Reserve University and the Cleveland Clinic in compliance with the Public Health Services Policy on humane care and use of animals.

In vitro slice preparation

Rodents were deeply anesthetized with isoflurane and decapitated. The brainstem was then removed in a 95% O_2, 5% CO_2 (carbogen)-gassed artificial cerebral spinal fluid with sucrose replacement of Na^+ to maintain osmolarity and prevent activity–induced cell death (Aghajanian and Rasmussen 1989) (S-ACSF; in millimolar, 250 sucrose, 3 KCl, 1.5 $CaCl_2$, 1 $MgSO_4$, 0.5 $NaHPO_4$, 25 $NaHCO_3$, 30 D-glucose). Transverse medullary slices were made on a VT1000 vibratome (Vibratome Instruments, St. Louis, MO), while continuously perfusing the tissue with chilled (3–6°C) carbogen gassed S-ACSF. Final slices of 300–400μM were cut to contain the commissural portion of the nTS for recording of individual nTS neurons. Following sectioning, the slice was placed in a polycarbonate chamber (26GLP, Warner instruments, Hamden, CT) and held in place with a platinum ring overlain with nylon threads. The slice was continually perfused with sodium-containing ACSF (in millimolar, 124 NaCl, 3 KCl, 1.5 $CaCl_2$, 1 $MgSO_4$, 0.5 $NaHPO_4$, 25 $NaHCO_3$, 30 D-glucose) bubbled with carbogen gas at 26–27°C for up to 6 hours. For visual targeting of patch pipettes the slice was imaged using an upright Leica DM/LFS microscope (Leica Microsystems GmBH, Wetzlar, Germany) and an infrared sensitive CCD camera (DAGE-MTI, Michigan City, IN).

Intracellular recording

Electrophysiologic studies focused on two regions: the nTS, where sensory afferent input is received and transmitted to autonomic reflex pathways critical for maintenance of respiratory function, including responses to hypoxia, and the VLM, which contains relay neurons for autonomic pathways. Patch pipettes (Borosilicate glass BF150, Sutter Instruments, Novato, CA), pulled to a 1.5–2μm tip diameter (Sutter Instruments P-97), were used to record from individual neurons in the commissural nTS. Patch pipettes were filled with intracellular solution (in millimolar, 130 K-gluconate, 10 Na-gluconate, 4 NaCl, 10

HEPES, 4 Mg-ATP, 0.3 GTP, 4 Na_2-phosphocreatine, pH 7.3). Additional slices were exposed to ACSF containing low extracellular calcium in which all other salts were the same concentration as for regular ACSF except for calcium which was lowered to 0.2 mM. In these slices, cells were patched with a pipette containing high buffered intracellular calcium solution containing (in millimolar 125 K-gluconate, 20 mM KCl, 1 Mg-ATP, 1 GTP, 10 HEPES, 1 EGTA, 0.7 $CaCl_2$) (Laumonnier et. al 2006). This resulted in an intracellular free calcium concentration of 400nM. Pipette resistance was 6.5–7.5MΩ before sealing onto an nTS neuron. Approximately 30mmHg positive pressure was applied to the pipette in solution to keep the tip clear using an N_2-fed Picospritzer (Parker-Hannafin, Cleveland, OH). After a tight seal (>2GΩ) was obtained, whole-cell mode was initiated by membrane rupture using ~20mmHg of mouth-applied negative pressure. Capacitance and series resistances were measured and compensated for using software (*P-Clamp* software suite) and transients were eliminated using automated and manual compensation (Multiclamp 700A amplifier, Molecular Devices, Sunnyvale, CA). Cells which exhibited large access resistance (>1GΩ) or large leak currents (>100pA) were discounted from further analysis. Injected current in the range from −5 to −100pA was used to maintain a baseline membrane potential of approximately −65mV. Recordings were performed in voltage-clamp (V-clamp) and voltage pulse protocols applied to evaluate I-V relationships (Fig. 1 panel A). Resting membrane potential was measured and corrected for junction potential which was 12.5 mV. We also recorded action potentials in current clamp in response to voltage injection. In one set of experiments, cells were held in current clamp at the minimum voltage to elicit action potential firing and recorded for 1 minute. We compared action potentials by averaging the first 10 spikes from each cell meeting the inclusion criteria, and using the peak of the action potential as a point of alignment. From these recordings, we analyzed the timing from baseline to peak of the action potential; peak of the action potential to the peak of the afterhyperpolarization (AHP); and from the minimum of the AHP to return to baseline. Return to baseline was defined as the point at which the membrane voltage first crossed the baseline after the peak of the AHP, provided that this was not the starting point of another action potential. If another action potential started immediately upon the return to baseline, this action potential was not included in analysis. Additionally, in a separate set of experiments, current pulses of increasing amplitude and 10ms duration were injected until the neuron fired at least a single action potential. This current, along with currents of 400 pA, and 1nA were then injected into the cell for 100ms for the construction of an I-frequency curve. Specific channel blockers for SK and BK channels (apamin 10nM, iberiotoxin 50μM final concentrations after Butcher et al. 1999, and Pedarzani et al. 2000), were added to the bath after the initial I-V protocol, and allowed to perfuse into the slice for 10 min. after which a second, identical, I-V protocol was administered, as well as recording of action potentials in current clamp in response to injected current. The drug was then washed out for one hour before patching subsequent cells.

Histology

Animals were perfused transcardially with ice-cold saline followed by ice cold 4% paraformaldehyde (PFA). The brain was then removed and post fixed in 4% PFA overnight, followed by cryoprotection with 30% sucrose for 24–48 hours. The medulla was then mounted in TFM tissue freezing medium (Triangle Biomedical Sciences, Durham, NC) and 10μm slices were cut on a cryostat (Leica CM 1800, Leica Microsystems GmbH, Wetzlar, Germany). Tissue sections were stored at −80°C until use. Tissue sections were treated with 0.01% H_2O_2 in phosphate buffered saline (PBS) for 30min. Followed by 1 hour in dilution buffer (DB) consisting of 0.03% Triton X-100 and 2% bovine serum albumin in PBS. Tissue sections were then incubated overnight in 1:200 Rabbit anti MBP (AB980, Millipore, Billerica, MA), 5% goat serum, and 0.1% Triton X-100 in PBS. Sections were then washed

3×5min. in DB, and incubated with 1:200 Goat and Rabbit biotin (Jackson Immunoresearch, West Grove, PA), 5% goat serum, and 0.01% Triton X-100 in PBS for 2 hours. Sections were then washed 3×10 min in PBS, and the staining visualized using the Preoxidase Standard Vectastain ABC Kit (PK-400, Vector Laboratories, Burlingame, CA) with 3, 3′–diaminobenzidine, and nickel enhancement. Slides were then dehydrated in alcohols and xylene, and coverslipped with Permount.

Photomicrographs were taken using a Leica DMLB microscope (Leica Microsystems GmbH, Wetzlar, Germany) and a Retiga Exi Camera (Q imaging, Surrey, BC, Canada). Images were captured with "Q Imaging" software.

Data Analysis

I-V plots were reconstructed for each cell using *Clampfit* software (Molecular Devices, Sunnyvale, CA) at two time points; the peak of the inward current (peak inward current), and 20ms after the onset of the voltage step (outward current). Current measurements were normalized for cell capacitance. Current clamp analysis was done using *Matlab* software v. 7.0.4 (Mathworks, Natick, MA) with code developed in-house. Data were compared between animals carrying gene mutations and littermate controls at each age using student's t-test and between age groups using individual one way-ANOVA (*SigmaStat* software). All data is presented as mean ± s.e.m.; p of <0.05 was considered significant.

3. Results

3.1 Properties of neurons in the nTS of MD rats, Plp^{msd} mice, and Plp^{null} mice at P20–24

First, we explored the membrane properties of neurons in the commissural nTS, the region of the caudal medulla which receives afferent input from the peripheral chemoreceptors. Figure 1 illustrates the area of study including the sites in nTS and the ventral lateral medulla (VLM). Interestingly, the nTS as seen in fig. 1B&C, is an area of the caudal medulla that remains unmyelinated at postnatal day 21 in the rat, in contrast to other areas of the brainstem such as VLM (Fig. 1D, Massari et al. 1996).

Using whole-cell patch-clamp in organotypic brainstem slices, we compared the cellular properties of neurons from rodents with three differing mutations in the *Plp* gene: MD rats, Plp^{msd} mice, and Plp^{null} mice, using their age-matched WT littermates as controls (Table 1). At P14–P16 there was a significantly lower resting membrane potential in nTS neurons of WT rats when compared to those from MD rats. However, at P20–24 we found no significant differences in membrane capacitance (C_m), membrane resistance (R_m), and resting membrane potential (V_m), between the rodents with mutation in the *Plp* gene and littermate WT controls (MD control n=46, MD n=59; Plp^{msd} control n=20, Plp^{msd} n=11; Plp^{null} control n=16, Plp^{null} n=16).

3.2 Current-Voltage relationships in Plp mutant rodents at P20–24

The current voltage relationships of MD, Plp^{msd}, Plp^{null}, and WT nTS cells were compared at P20–24 by generating I-V curves for all groups. When we analyzed the peak inward current, we found no significant difference between cells from *Plp* mutants and WT animals at all voltage steps examined (Fig. 2). However, analysis of the outward current of the I-V curve taken 20ms after the onset of the voltage pulse, (primarily due to the outward flux of K^+ (Hodgkin and Huxley 1952), revealed a significantly decreased outward current in cells from *Plp* mutant animals when compared to cells from WT rodents (Fig. 2) (MD control n=16, MD n=25; Plp^{msd} control n=20, Plp^{msd} n=11; Plp^{null} control n=16, Plp^{null} n=16). These findings show that different mutations in the *Plp* gene, as well as absence of PLP/

DM20 in the transgenic *Plp* null mouse, result in a very similar defect in the ability of neuronal membranes to repolarize after a prolonged depolarizing transient.

In addition, injection of the minimum current into each cell necessary to elicit action potential firing revealed similar abnormalities in the repolarization phase of the action potential in MD (Fig. 3), Plp^{msd} and Plp^{null} nTS cells when compared to WT cells. Neurons from P20–24MD, Plp^{msd}, and Plp^{null} animals had significantly reduced area of the AHP (Area: MD = 5007 ± 962V•s; WT = 7676 ± 996V•s, $p < 0.034$: Plp^{msd} = 5475 ± 651V•s; Plp^{WT} = 7926 ± 1185V•s, $p < 0.035$: Plp^{null} = 5656 ± 777V•s; Plp^{WT} = 8680 ± 1363V•s, $p < 0.039$) when compared to cells from WT littermates (Fig. 3A&B). Additionally, cells from P20–24MD rats and Plp^{null} mice took significantly longer to return to baseline from the peak of the AHP when compared to WT (MD = 0.087 ± 0.003s; WT = 0.077 ± 0.003s, $p < 0.036$: Plp^{null} = 0.089 ± 0.006s; Plp^{WT} = 0.074 ± 0.005s, $p < 0.039$) (Fig. 3C).

In Plp^{msd} mice nTS cells required a significantly shorter time to reach the peak AHP after the peak of the action potential (Plp^{msd} = 0.020 ± 0.003s; Plp^{WT} = 0.027 ± 0.001s, $p < 0.016$) when compared to WT (Fig. 3D). This abnormality was not present in neurons from MD rats or Plp^{null} mice.

No alteration was detected in the timing from onset of the action potential to the peak in any of these three animal models (MD $p < 0.09$; Plp^{msd} $p < 0.33$; Plp^{null} $p < 0.15$). Thus, the current contributing to the peak of the action potential itself was not altered in the nTS of any of the *plp* mutants in this study.

We speculated that the abnormality in afterhyperpolarization found in the rodents with mutation in the *Plp* gene could potentiate action potential firing (Pedarzani et al. 2000; Zhang et al. 2003). We found that there was no significant difference in the rheobase between *plp* mutant and WT nTS neurons at P20–24 (MD = 47.8 ± 10.4 pA; WT = 54.77 ± 11.03 pA, $p < 0.33$: Plp^{msd} = 42.54 ± 8.49 pA; Plp^{WT} = 30.56 ± 5.57 pA, $p < 0.18$: Plp^{null} = 33.36 ± 5.46 pA; Plp^{WT} = 45.58 ± 8.17 pA, $p < 0.44$). When we injected the minimum current in order to elicit spiking into MD and WT nTS neurons for 100ms we saw no significant difference in the number of spikes fired. Also, at high levels of stimulation, 1nA, there was no significant difference in the numbers of spikes elicited between MD and WT, as both groups fired only a few spikes at the very onset of stimulation. However, a current pulse of 400pA for 100ms elicited trains of spikes in both groups with significantly more spikes in MD neurons compared to WT (MD = 9.1 ± 0.95spikes; WT = 5.8 ± 1.1spikes, $p < 0.017$). Thus, mutation in the *Plp* gene increased the frequency of firing of nTS neurons during spike trains.

3.3 Electrophysiology of the VLM in the MD rat

In order to determine whether the effects of *Plp* mutation on outward current were truly specific and isolated to the nTS, we recorded from neurons in the ventrolateral medulla (VLM) in the MD rat. As is seen in Fig. 1B&D, using antibodies against MBP, this area is heavily myelinated at P21 in the rat, in contrast to the nTS. As we had observed in the nTS neurons of MD rats, the neurons from the VLM also exhibited significantly decreased outward current when compared to VLM cells from WT ($p < 0.0005$) (Fig. 4B). In addition, a significant increase in peak inward current ($p < 0.05$ for all voltage steps) was seen in VLM cells from MD animals (n=11) when compared to WT VLM cells (n=10) (Fig. 4A). Thus, VLM neurons differed from nTS neurons in that both the peak inward current and outward current were significantly affected. This suggests that the neuronal effects of *Plp* gene mutation may differ between areas of the caudal medulla, possibly reflecting the underlying influence of extent of myelination in the area.

3.4 Electrophysiology in the myelin deficient Mbp^{shi} mouse

The complex structure of myelin includes PLP as well as other proteins such as myelin basic protein (MBP). Conceivably, mutation in any of the proteins present in myelin could alter the properties of neurons in the CNS. Therefore, to determine if the defect in cellular repolarization seen in the rodents with *Plp* gene mutation was specific to the mutation of PLP, or could be a general phenomenon of dysmyelination, we studied the cellular properties of nTS cells in the *Mbp^{shi}* mouse at P21–25. The *Mbp^{shi}* mouse has a mutation in the MBP gene, which results in CNS dysmyelination, however these mice do not exhibit seizures or early death as found in the rodents with *Plp* mutation. Furthermore, we have shown that the *Mbp^{shi}* mouse has a normal ventilatory response to hypoxia (Miller et al. 2004).

We observed that the R_m and C_m in cells from *Mbp^{shi}* (n=26) and WT (n=20) littermates did not differ significantly, while the V_m was more negative in *Mbp^{shi}* cells when compared to cells from WT ($p < 0.002$) (Table 1). The peak inward current in response to positive voltage steps was significantly reduced in *Mbp^{shi}* nTS neurons at P21 ($p < 0.05$) at steps above −10mV (Fig. 4C) while the outward current did not differ significantly ($p > 0.10$ at all voltage steps) (Fig. 4D). We saw no significant difference in rheobase values in cells from mutant and WT animals (*Mbp^{shi}* = 81.1 ± 22.6 pA; *Mbp^{WT}* = 73.19 ± 15.1 pA; $p < 0.38$). In addition, during current clamp, there was no significant change in the area of the AHP ($p < 0.44$) or in the timing of the action potential peak or the AHP (baseline to peak $p < 0.059$; peak to minimum $p < 0.18$; minimum to baseline $p < 0.28$) (Fig 3B–D). Thus dysmyelination as occurs in the *Mbp^{shi}* mouse does not alter outward current in nTS neurons; instead, this mutation alters the ionic currents contributing to peak inward current.

3.6 Age dependence of neuronal properties in the MD rat

In our previous study (Miller et al. 2003), we observed that the ventilatory response to hypoxia was normal in MD rats at P12–14, but these animals exhibited lethal hypoxic ventilatory depression by P20–24. In order to determine if the electrophysiological abnormalities in the MD rat were age specific, we examined cellular and current characteristics in nTS neurons from the MD rat at P12–14. We found that both C_m ($p < 0.38$) and R_m ($p < 0.47$) were not significantly different in nTS cells from MD and WT littermates at P12–14. Interestingly, at P12–14, the resting membrane potential (V_m) of cells from WT rats was significantly lower when compared to cells from MD rats (Table 1; $p < 0.005$) a difference which was not present at P20–24.

In contrast to the findings in the P20–24 MD rat, we saw no differences in peak inward current or outward current at any voltage step tested between cells from MD and WT animals at P12–14 (peak $p > 0.13$; outward $p > 0.21$) (Fig. 5). Furthermore, in WT rats we observed that an increase in outward current normally occurred after P12–14 and before P20–24. The MD rat failed to show this normal maturational change in outward current. (Fig. 5, P14 MD control n=27; P14 MD n=36).

When we examined the properties of the action potentials from P12–14 MD rats using current clamp we again saw no deficits when compared to WT in either the area of the AHP ($p < 0.38$) or the timing of the action potential (baseline to peak $p < 0.27$; peak to minimum $p < 0.31$; minimum to baseline $p < 0.20$) (Fig. 3B–D). These results indicate that the nTS MD neurons exhibited a developmental defect in the ability to generate outward current.

3.7 Selective Channel blockade in the MD rat

The afterhyperpolarization in CNS neurons depends on activation of a number of channels including calcium channels, calcium-dependent potassium channels, and voltage activated

K^+ channels. Because we observed deficits in the time required to return to baseline from the peak of the AHP, we tested the hypothesis that contribution of small conductance (SK) and large conductance (BK) calcium-dependent potassium channels to the outward current would be abnormal in the MD rat. These channels operate on a longer time scale than delayed rectifier voltage-gated potassium channels and play a major role in this phase of the AHP. These Ca^{2+} dependent K^+ channels contribute to regulation of the spontaneous firing frequency and shape of single action potentials of neurons (Sah 1996; Pedarzani et al. 2000).

We focused these studies on the MD rat as a model; for we had observed that all rodents with *Plp* mutation exhibited a similar defect in outward current during afterhyperpolarization (see above). In order to examine the contribution of SK channels to neuronal repolarization in the MD rat, we compared current–voltage relationships in cells from MD and WT rats before and after SK channel blockade by bath application of 10nM apamin (Butcher et al. 1999; Laumonnier et al. 2006) at both P12–14 (control n=8, MD n=9) and P20–24 (n=8 all groups). We observed a significant decrease in outward current after application of apamin at voltage steps above −10mV in nTS neurons from WT rats at P20–24 ($p < 0.05$ at steps above −10mV) but not at P12–14 ($p > 0.37$ at all voltage steps) (Fig. 6 A&C). However, the neurons from MD animals exhibited no significant change in outward current in response to apamin in either age at any voltage step (P21 $p > 0.19$; P14 $p > 0.08$ for all voltage steps) (Fig. 6A). Therefore, we conclude that SK channels are active by P20–24 in WT animals in the nTS, but not at P12–14, and more importantly, that SK channels fail to contribute significantly to outward current in the MD rat. In order to confirm this finding, we examined action potentials in current clamp, both with and without apamin in WT rats at P21, and saw a significant decrease of 5mV in membrane voltage during the AHP ($p < 0.007$) (Fig. 6E left panel). However, in neurons from MD rats, apamin did not alter the AHP ($p < 0.13$) indicating undetectable SK channel function in these neurons. (Fig. 6E right panel)

Additionally, we examined the contribution of BK channels to outward current in the nTS of MD and WT rats by application of 50μM iberiotoxin (Pedarzani et al. 2000) (Fig. 6B&D) at P12–14 and P20–24. No effect of iberiotoxin was observed in neurons from P12–14 WT animals (n=10; $p > 0.16$). However, a significant decrease in outward current was seen after application of iberiotoxin in neurons from control rats at P20–24 (n= 9; $p < 0.04$) at voltage steps above −10mV. In MD rats we observed no effect of iberiotoxin on outward currents at either P12–14 (n=9; $p > 0.11$) or P20–24 (n=12; $p > 0.22$) at any voltage step tested. These results show that the contribution of both SK and BK channels to outward current in nTS neurons normally undergoes a significant maturational increase between P12–14 and P20–24 which does not occur in MD rats.

Similarly, when we examined action potentials under current clamp, both with and without iberiotoxin in WT rats at P21, we saw a significant reduction in the AHP of 3mV ($p < 0.04$) (Fig. 6F left panel). However, in cells from MD rats there was no significant decrease in the voltage during the AHP in response to iberiotoxin treatment ($p < 0.11$) again indicating undetectable BK channel function in these cells (Fig. 6F right panel).

3.8 The role of calcium in the MD phenotype

BK and SK channels require both proper voltage-gating and calcium binding in order to function. In order to determine if the lack of BK and SK channel involvement in nTS neurons from MD rats was truly due to a lack of function of these channels or was secondary to altered calcium dynamics, we obtained whole-cell recordings from nTS cells in both WT and MD rats using a buffered high intracellular calcium and low extracellular calcium (Laumonnier et. al 2006). This procedure was designed to compensate for any potential deficit in calcium entry in these cells in the MD rat, and would allow complete activation of BK and SK channels. When we examined the outward current, we saw no significant

difference between the current voltage relationships of MD nTS cells when exposed to either normal or high intracellular calcium ($p > 0.10$ for all voltage steps) (Fig. 7A). Thus, high intracellular calcium did not correct the defect in outward current observed in nTS cells from MD rats.

When we characterized the action potential of MD and control nTS cells under current clamp we saw no significant differences in the timing of the AP and AHP between recordings made under high intracellular and low extracellular calcium and those made under normal ionic conditions (Fig. 7B). Furthermore, the abnormal AHP seen in MD nTS neurons persisted even in the presence of high intracellular calcium. Thus provision of increased calcium availability failed to correct the deficits in SK and BK function which we observed in nTS neurons from P21 MD rats.

4. Discussion

The major finding of this study is that mutation in a gene normally associated with CNS myelin can alter the electrophysiologic properties of neurons in the caudal medulla. The proteolipid protein gene is located on the X-chromosome, and is remarkably conserved across mammalian species; at the amino acid level there is complete homology between mouse and man (Dautigny et al. 1985; Schweitzer et al. 2006). The major transcript of this gene in the CNS is proteolipid protein, a lipophilic protein which is the principal component of compact myelin and has non-structural functions in the cell, for PLP has also been found to be a component of membrane complexes involving αV integrin in the oligodendrocyte (Gudz et al. 2002). In addition to *Plp* expression in oligodendrocytes, our recent studies and those of others have verified the presence of PLP mRNA and protein in neurons in the CNS, including the caudal medulla of the developing rodent (Bongarzone et al. 1999; Jacobs et al. 2003, 2004; Miller et al. 2003, 2009; Greenfield et al. 2006). Because we have documented *Plp* promoter, Plp mRNA and PLP protein expression in the caudal medulla we hypothesized that this gene could play a heretofore unknown functional role in neurons in this area.

4.1 Normal development of afterhyperpolarization is prevented by mutation in the Plp gene

In this study, we observed that rodents with 3 different alterations in the *Plp* gene developed similar dysfunction of outward current in the nucleus tractus solitarius. This finding appears to be unique to rodents with *Plp* mutations, for the shiverer mouse, which has a dysmyelinating mutation in the myelin basic protein gene, did not exhibit alteration of afterhyperpolarization. Additionally, we demonstrated that BK and SK channels contribute to this dysfunction in the MD rat.

BK and SK channels are critical for generation of hyperpolarizing outward current in neurons. The alteration of membrane repolarization due to BK and SK channel dysfunction in the MD rat was noted to be age dependent, occurring in the third week of life. From our data, it appears that mutation in the *Plp* gene interrupts the normal development of BK and SK channel function in the area of the commissural nTS in the medulla. This area is important for processing sensory afferent input from the peripheral chemoreceptors (Finley and Katz, 1992). Hypothetically, alteration of these channels could change the central response to input from the carotid chemoreceptors. Carotid chemoreceptor afferent neurons innervate the commissural subnucleus of the nTS (Finley and Katz, 1992; Housley et al. 1987). This subnucleus contains glutamatergic, and to a lesser extent gabaergic neurons which, in turn, innervate the CO_2 sensitive neurons of the RTN, an area which functions as a central integrator of central and peripheral chemoreceptor input (Bodineau et al. 2000, Guyenet, et al. 2008, Takakura, et al. 2006). Thus, at the critical age (P19–21) two pathophysiologic changes occur in the *Plp* mutant rodents; onset of seizures, and

development of abnormal response to hypoxia. Hypothetically, hypoxia could develop during sleep, or during seizures. In animals with mutation in the *Plp* gene, failure of hyperpnea during hypoxia could be due to decreased drive from the nTS to the retrotrapezoid nucleus and other areas, leading to subsequent terminal apnea.

One drawback of this study was that we did not directly measure neuronal response to stimulation of the afferent pathway itself, the tractus solitarius or to stimulation of the carotid sinus nerve. This will be necessary, in future studies, to determine in more detail how afferent sensory input in this reflex system is altered by mutation in the proteolipid protein gene.

4.2 Charateristics of neurons differed in myelinated and unmyelinated areas of the caudal medulla in the MD rat

The electophysiologic characteristics of neurons in the MD rat were observed to differ between the nTS, an area that is unmyelinated, and the VLM, where myelination is extensive at P21 (Fig. 1). In the nTS, peak inward current was normal; however, outward current was diminished. In the VLM, we observed an increase in peak inward current and decreased outward current. These observations suggest that more than one mechanism may be at work in alteration of axonal or somatic membrane channels in myelinated areas of the CNS due to *Plp* mutation.

4.3 Mechanisms of disruption of BK and SK channel function

BK and SK channels are composed of multiple tissue-specific subunits which are contained in interdependent cell membrane complexes composed of specific proteins, including ion channels and signalling proteins (Berkefeld et al. 2006; Lu et al. 2006; Pedarzani and Stocker 2008). Mutation in the *Plp* gene could alter BK and SK channel function in the neuron by several mechanisms including disruption of normal oligodendrocyte-neuronal interaction (Lappe-Siefke et al. 2003), expression of a toxic misfolded gene product within the neuron itself (Gow A et al, 1994, 1996), or downregulation of other gene products (Yanagisawa et al. 1986) In preliminary studies (unpublished) we have found that BK α, BK β, and SK α channel subunit protein content was not altered (as measured by immunoblot), in the caudal medulla from MD and WT rats at P21. Furthermore, we found no difference when we compared immunostaining for these proteins in neurons in the caudal medulla of the MD and WT rat. Therefore, the dysfunction of BK and SK channels due to *Plp* mutation does not appear to be simply due to down-regulation of channel subunit expression.

BK and SK channel activation is dependent on an increase in intracellular calcium, via voltage gated calcium channels. Hypothetically, the dysfunction in BK and SK channels could have been due to impairment of calcium entry into the cell. In this study we found that the impairment of BK and SK channel function was not changed in the presence of high intracellular calcium. This finding does not however rule out a defect in intracellular access to free calcium or impaired calcium mobility.

In earlier work on the MD rat, mutation in the *Plp* gene was found to be associated with disorganization of myelin and axonal channels and associated proteins. Specifically, lack of clustering of contactin, Caspr and NF155, as well as aberrant localization of Kv1.1 and Kv1.2 was observed in the spinal cord (Arroyo et al. 2002) and decreased axonal sodium channel clustering was observed in the optic nerve of the MD rat (Kaplan et al. 1997). Therefore, it is possible that the functional organization of the synaptic complexes containing these channels and their distribution within the neural membrane is altered by mutation in the *Plp* gene. Wu et al. (2008) have shown that $\alpha_v\beta_1$ integrin activation potentiates BK channel activity in vascular smooth muscle. Furthermore, our laboratory has

shown that PLP functions as part of an α_v integrin signalling complex in oligodendrocytes and that AMPA mediated induction of oligodendrocyte progenitor migration did not occur in oligodendrocytes from the MD rat (Gudz et al. 2002, 2006) Further work will be needed to establish whether, indeed, PLP functions in concert with integrin receptors in the neuron, and how this is linked to ion channel regulation.

Our observation that the *Plp* null mouse, which expresses no PLP protein, also exhibits diminished afterhyperpolarization further supports the concept that the presence of PLP protein during development is critical for normal function of BK and SK channels in the neuron. However, this finding cannot explain the early death, seizures, and abnormal response to hypoxia observed in the MD rat and the Plp^{msd} mouse, for the null mutant exhibits none of the major pathophysiologic characteristics conferred by *Plp* mutations, although it does exhibit abnormalities in myelin ultrastructure (Klugmann et al. 1997; Rosenbluth et al. 2006).

Our study was limited to calcium dependent potassium channels, which are involved in afterhyperpolarization following action potential discharge, in the caudal medulla. It is conceivable that other channels and their membrane-associated complexes could be altered, depending on degree of myelination and the region of the CNS examined. Further studies of the molecular architecture of the CNS synapse in the rodents with *Plp* mutation could shed additional light on the mechanisms by which BK and SK channel function is disturbed.

4.4 Implications for Pelizaeus-Merzbacher disease

Mutations in the *Plp* gene provide genetic models for Pelizaeus-Merzbacher disease, a severe leukoencephalopathy characterized by nystagmus, hypotonia, ataxia, spasticity, seizures and mental retardation (Seitelberger 1995). The early severe form (connatal) of Pelizaeus Merzbacher disease can result in seizures and death within the first decade of life. Traditionally, the phenotype of these patients has been attributed to a lack of myelin and therefore, impaired neural transmission in the brain. The present study and our earlier studies (Miller et al. 2003, 2004) raise the possibility that *Plp* mutation could directly influence neuronal function in diverse areas of the CNS of these patients. For example, in *in vitro* models of epilepsy, down regulation of SK channel mediated afterhyperpolarization was observed to parallel the emergence of epileptiform activity (Fernandez de Sevilla et al. 2006). Other groups have shown that an absence of BK channel function due to knockout of the BK gene results in ataxia (Sausbier et al. 2004). Thus we speculate that, if altered BK and SK channel function occurs in other areas of the CNS, this could underlie the pathophysiologic ataxia and seizures in Pelizaeus-Merzbacher patients. If so, pharmacologic intervention targeting these channels could be of future benefit in this devastating disease.

Acknowledgments

The authors would like to thank Paulina Getsy and Daniel Niedzwiecki for help in data collection for this manuscript.

Grants This research was supported by grants from the National Multiple Sclerosis Society RG3669 (MJM) and the NIH, NS25304 (WBM).

References

Aghajanian GK, Rasmussen K. Intracellular studies in the facial nucleus illustrating a simple new method for obtaining viable motoneurons in adult rat brain slices. Synapse. 1989; 3:331–338. [PubMed: 2740992]

Arroyo EJ, Xu T, Grinspan J, Lambert S, Levinson SR, Brophy PJ, Peles E, Scherer SS. Genetic dysmyelination alters the molecular architecture of the nodal region. J. Neurosci. 2002; 22:1726–1737. [PubMed: 11880502]

Berkefeld H, Sailer CA, Bildl W, Rohde V, Thumfart JO, Eble S, Klugbauer N, Reisinger E, Bischofberger J, Oliver D, Knaus HG, Schulte U, Fakler B. BKCa-Cav channel complexes mediate rapid and localized Ca2+-activated K+ signaling. Science. 2006; 314:615–620. [PubMed: 17068255]

Bodineau L, Frugière A, Marlot D, Wallois F. Connections between retrotrapezoid nucleus and nucleus tractus solitarii in cat. Neurosci. Lett. 2000; 280:111–114. [PubMed: 10686390]

Bongarzone ER, Campagnoni CW, Kampf K, Jacobs EC, Handley VW, Schonmann V, Campagnoni AT. Identification of a new exon in the myelin proteolipid protein gene encoding novel protein isoforms that are restricted to the somata of oligodendrocytes and neurons. J. Neurosci. 1999; 19:8349–8357. [PubMed: 10493736]

Boulloche J, Aicardi J. Pelizaeus-Merzbacher disease: clinical and nosological study. J. Child. Neurol. 1986; 1:233–239. [PubMed: 3598129]

Butcher JW, Kasparov S, Paton JF. Differential effects of apamin on neuronal excitability in the nucleus tractus solitarii of rats studied in vitro. J. Auton. Nerv. Syst. 1999; 77:90–97.

Ciriello J, Hrycyshyn AW, Calaresu FR. Horseradish peroxidase study of brain stem projections of carotid sinus and aortic depressor nerves in the cat. J. Auton. Nerv. Syst. 1981; 4:43–61. [PubMed: 7264203]

Csiza CK, deLahunta A. A neurologic mutant in the wistar rat. Am. J. Pathol. 1979; 95:215–224. [PubMed: 434110]

Dautigny A, Alliel PM, d'Auriol L, Pham Dinh D, Nussbaum JL, Galibert F, Jolles P. Molecular cloning and nucleotide sequence of a cDNA clone coding for rat brain myelin proteolipid. FEBS Lett. 1985; 188:33–36. [PubMed: 2410294]

Dentinger MP, Barron KD, Csiza CK. Ultrastructure of the central nervous system in a myelin deficient rat. J. Neurocytol. 1982; 11:671–691. [PubMed: 7131049]

Fernandez de Sevilla D, Garduno J, Galvan E, Buno W. Calcium-activated afterhyperpolarizations regulate synchronization and timing of epileptiform bursts in hippocampal CA3 pyramidal neurons. J. Neurophysiol. 2006; 96:3028–3041. [PubMed: 16971683]

Finley JC, Katz DM. The central organization of carotid body afferent projections to the brainstem of the rat. Brain Res. 1992; 572:108–116. [PubMed: 1611506]

Garbern J, Cambi F, Shy M, Kamholz J. The molecular pathogenesis of Pelizaeus-Merzbacher disease. Arch. Neurol. 1999; 56:1210–1214. [PubMed: 10520936]

Gencic S, Hudson LD. Conservative amino acid substitution in the myelin proteolipid protein of jimpymsd mice. J. Neurosci. 1990; 10:117–124. [PubMed: 1688931]

Gow A, Friedrich VL Jr. Lazzarini RA. Many naturally occurring mutations of myelin proteolipid protein impair its intracellular transport. J. Neurosci. Res. 1994; 37:574–583. [PubMed: 7518006]

Gow A, Lazzarini RA. A cellular mechanism governing the severity of Pelizaeus-Merzbacher disease. Nat. Genet. 1996; 13:422–428. [PubMed: 8696336]

Greenfield EA, Reddy J, Lees A, Dyer CA, Koul O, Nguyen K, Bell S, Kassam N, Hinojoza J, Eaton MJ, Lees MB, Kuchroo VK, Sobel RA. Monoclonal antibodies to distinct regions of human myelin proteolipid protein simultaneously recognize central nervous system myelin and neurons of many vertebrate species. J. Neurosci. Res. 2006; 83:415–431. [PubMed: 16416423]

Gudz TI, Komuro H, Macklin WB. Glutamate stimulates oligodendrocyte progenitor migration mediated via an alphav integrin/myelin proteolipid protein complex. J. Neurosci. 2006; 26:2458–2466. [PubMed: 16510724]

Gudz TI, Schneider TE, Haas TA, Macklin WB. Myelin proteolipid protein forms a complex with integrins and may participate in integrin receptor signaling in oligodendrocytes. J. Neurosci. 2002; 22:7398–7407. [PubMed: 12196561]

Guyenet PG. The 2008 Carl Ludwig Lecture: retrotrapezoid nucleus, CO2 homeostasis, and breathing automatically. J. Appl. Physiol. 2008; 105:404–416. [PubMed: 18535135]

Hodgkin AL, Huxley AF. Currents carried by sodium and potassium ions through the membrane of the giant axon of Loligo. J. Physiol. 1952; 116:449–472. [PubMed: 14946713]

Housley GD, Martin-Body RL, Dawson NJ, Sinclair JD. Brainstem projections of the glossopharyngeal nerve and its carotid sinus branch in the rat. Neuroscience. 1987; 22:237–50. [PubMed: 3627444]

Jacobs EC, Bongarzone ER, Campagnoni CW, Campagnoni AT. Embryonic expression of the soma-restricted products of the myelin proteolipid gene in motor neurons and muscle. Neurochem. Res. 2004; 29:997–1002. [PubMed: 15139298]

Jacobs EC, Bongarzone ER, Campagnoni CW, Kampf K, Campagnoni AT. Soma-restricted products of the myelin proteolipid gene are expressed primarily in neurons in the developing mouse nervous system. Dev. Neurosci. 2003; 25:96–104. [PubMed: 12966208]

Kaplan MR, Meyer-Franke A, Lambert S, Bennett V, Duncan ID, Levinson SR, Barres BA. Induction of sodium channel clustering by oligodendrocytes. Nature. 1997; 386:724–728. [PubMed: 9109490]

Klugmann M, Schwab MH, Puhlhofer A, Schneider A, Zimmermann F, Griffiths IR, Nave KA. Assembly of CNS myelin in the absence of proteolipid protein. Neuron. 1997; 18:59–70. [PubMed: 9010205]

Knapp PE. Proteolipid protein: is it more than just a structural component of myelin? Dev. Neurosci. 1996; 18:297–308. [PubMed: 8911768]

Kumar S, Macklin WB, Gordon MN, Espinosa de los Monteros A, Cole R, Scully SA, de Vellis J. Transcriptional regulation studies of myelin-associated genes in myelin-deficient mutant rats. Dev. Neurosci. 1990; 12:316–325. [PubMed: 1705212]

Lappe-Siefke C, Goebbels S, Gravel M, Nicksch E, Lee J, Braun PE, Griffiths IR, Nave KA. Disruption of Cnp1 uncouples oligodendroglial functions in axonal support and myelination. Nat. Genet. 2003; 33:366–374. [PubMed: 12590258]

Laumonnier F, Roger S, Guerin P, Molinari F, M'Rad R, Cahard D, Belhadj A, Halayem M, Persico AM, Elia M, Romano V, Holbert S, Andres C, Chaabouni H, Colleaux L, Constant J, Le Guennec JY, Briault S. Association of a functional deficit of the BKCa channel, a synaptic regulator of neuronal excitability, with autism and mental retardation. Am. J. Psychiatry. 2006; 163:1622–1629. [PubMed: 16946189]

Lu R, Alioua A, Kumar Y, Eghbali M, Stefani E, Toro L. MaxiK channel partners: physiological impact. J. Physiol. 2006; 570:65–72. [PubMed: 16239267]

Massari VJ, Shirahata M, Johnson TA, Gatti PJ. Carotid sinus nerve terminals which are tyrosine hydroxylase immunoreactive are found in the commissural nucleus of the tractus solitarius. J. Neurocytol. 1996; 25:197–208. [PubMed: 8737172]

Meier H, MacPike AD. A neurological mutation (msd) of the mouse causing a deficiency of myelin synthesis. Exp. Brain Res. 1969; 10:512–25. [PubMed: 5433413]

Miller MJ, Haxhiu MA, Georgiadis P, Gudz TI, Kangas CD, Macklin WB. Proteolipid protein gene mutation induces altered ventilatory response to hypoxia in the myelin-deficient rat. J. Neurosci. 2003; 23:2265–2273. [PubMed: 12657685]

Miller MJ, Haxhiu MA, Kangas CD, Georgiadis P, Gudz TI, Macklin WB. Selective alteration of the ventilatory response to hypoxia results from mutation in the myelin proteolipid protein gene. Adv. Exp. Med. Biol. 2004; 551:85–91. [PubMed: 15602948]

Miller MJ, Kangas CD, Macklin WB. Neuronal expression of the proteolipid protein gene in the medulla of the mouse. J. Neurosci. Res.. 2009 doi:10.1002/jnr.22121.

Panneton WM, Loewy AD. Projections of the carotid sinus nerve to the nucleus of the solitary tract in the cat. Brain Res. 1980; 191:239–244. [PubMed: 7378754]

Pedarzani P, Kulik A, Muller M, Ballanyi K, Stocker M. Molecular determinants of Ca2+-dependent K+ channel function in rat dorsal vagal neurones. J. Physiol. 2000; 527(Pt 2):283–290. [PubMed: 10970429]

Pedarzani P, Stocker M. Molecular and cellular basis of small--and intermediate-conductance, calcium-activated potassium channel function in the brain. Cell. Mol. Life Sci. 2008; 65:3196–3217. [PubMed: 18597044]

Prabhakar NR. Oxygen sensing by the carotid body chemoreceptors. J. Appl. Physiol. 2000; 88:2287–95. [PubMed: 10846047]

Readhead C, Hood L. The dysmyelinating mouse mutations shiverer (shi) and myelin deficient (shimld). Behav. Genet. 1990; 20:213–34. [PubMed: 1693848]

Rosenbluth J. Abnormal axoglial junctions in the myelin-deficient rat mutant. J. Neurocytol. 1987; 16:497–509. [PubMed: 3681351]

Rosenbluth J, Nave KA, Mierzwa A, Schiff R. Subtle myelin defects in PLP-null mice. Glia. 2006; 54:172–182. [PubMed: 16802387]

Sah P. Ca(2+)-activated K+ currents in neurones: types, physiological roles and modulation. Trends Neurosci. 1996; 19:150–154. [PubMed: 8658599]

Sausbier M, Hu H, Arntz C, Feil S, Kamm S, Adelsberger H, Sausbier U, Sailer CA, Feil R, Hofmann F, Korth M, Shipston MJ, Knaus HG, Wolfer DP, Pedroarena CM, Storm JF, Ruth P. Cerebellar ataxia and Purkinje cell dysfunction caused by Ca2+-activated K+ channel deficiency. Proc. Natl. Acad. Sci. U. S. A. 2004; 101:9474–9478. [PubMed: 15194823]

Schweitzer J, Becker T, Schachner M, Nave KA, Werner H. Evolution of myelin proteolipid proteins: gene duplication in teleosts and expression pattern divergence. Mol. Cell. Neurosci. 2006; 31:161–177. [PubMed: 16289898]

Seitelberger F. Neuropathology and genetics of Pelizaeus-Merzbacher disease. Brain Pathol. 1995; 5:267–273. [PubMed: 8520726]

Simons R, Riordan JR. Single base substitution in codon 74 of the MD rat myelin proteolipid protein gene. Ann. N. Y. Aca.d Sci. 1990; 605:146–154.

Takakura AC, Moreira TS, Colombari E, West GH, Stornetta RL, Guyenet PG. Peripheral chemoreceptor inputs to retrotrapezoid nucleus (RTN) CO2-sensitive neurons in rats. J. Physiol. 2006; 572:503–523. [PubMed: 16455687]

Tosic M, Gow A, Dolivo M, Domanska-Janik K, Lazzarini RA, Matthieu JM. Proteolipid/DM-20 proteins bearing the paralytic tremor mutation in peripheral nerves and transfected Cos-7 cells. Neurochem. Res. 1996; 21:423–430. [PubMed: 8734435]

Tosic M, Matthey B, Gow A, Lazzarini RA, Matthieu JM. Intracellular transport of the DM-20 bearing shaking pup (shp) mutation and its possible phenotypic consequences. J. Neurosci. Res. 1997; 50:844–852. [PubMed: 9418971]

Wu X, Yang Y, Gui P, Sohma Y, Meininger GA, Davis GE, Braun AP, Davis MJ. Potentiation of large conductance, Ca2+-activated K+ (BK) channels by alpha5beta1 integrin activation in arteriolar smooth muscle. J. Physiol. 2008; 586:1699–1713. [PubMed: 18218680]

Yanagisawa K, Duncan ID, Hammang JP, Quarles RH. Myelin-deficient rat: analysis of myelin proteins. J. Neurochem. 1986; 47:1901–1907. [PubMed: 2430065]

Yool DA, Edgar JM, Montague P, Malcolm S. The proteolipid protein gene and myelin disorders in man and animal models. Hum. Mol. Genet. 2000; 9:987–992. [PubMed: 10767322]

Zhang XF, Gopalakrishnan M, Shieh CC. Modulation of action potential firing by iberiotoxin and NS1619 in rat dorsal root ganglion neurons. Neuroscience. 2003; 122:1003–1011. [PubMed: 14643767]

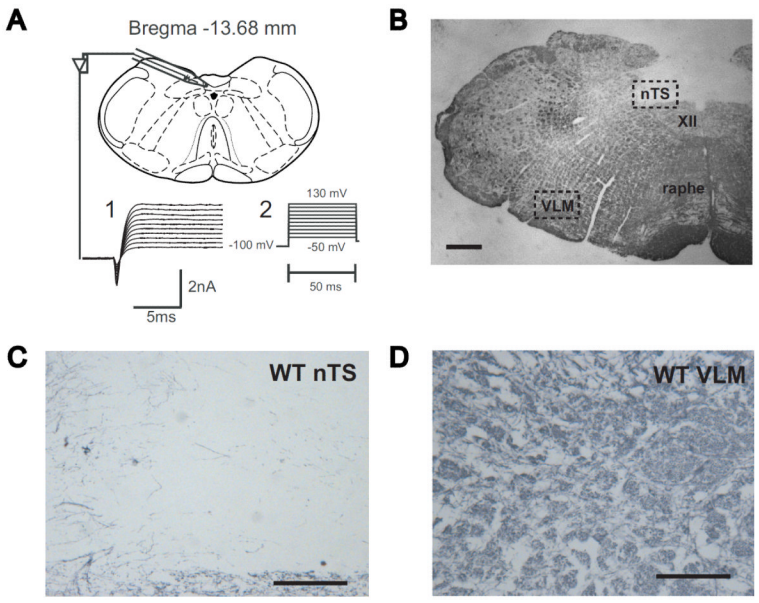

Figure 1.

A: Schematic showing the position of the recording electrode at the level of the commissural nTS, 1. A sample of the raw recording of the current evoked during the stimulus protocol. 2. The stimulus protocol applied during I-V recording from single nTS cells. This recording is from an nTs cell from a WT control rat. B: Section of the caudal medulla immunostained for myelin basic protein at P21 in the WT rat at 5x magnification. Dashed boxes indicate high magnification areas seen in panels C and D. Scale bar = 400μm C: High magnification (40x) view of the commissural nTS stained for MBP at P21. Very few myelinated fibers are seen in this area of the caudal medulla. Scale bar = 100μm. D: High magnification (40x) view of the ventral lateral medulla (VLM). In contrast to the nTS, many myelinated fibers are seen in this area of the caudal medulla. Scale bar = 100μm. XII=Hypoglossal nucleus.

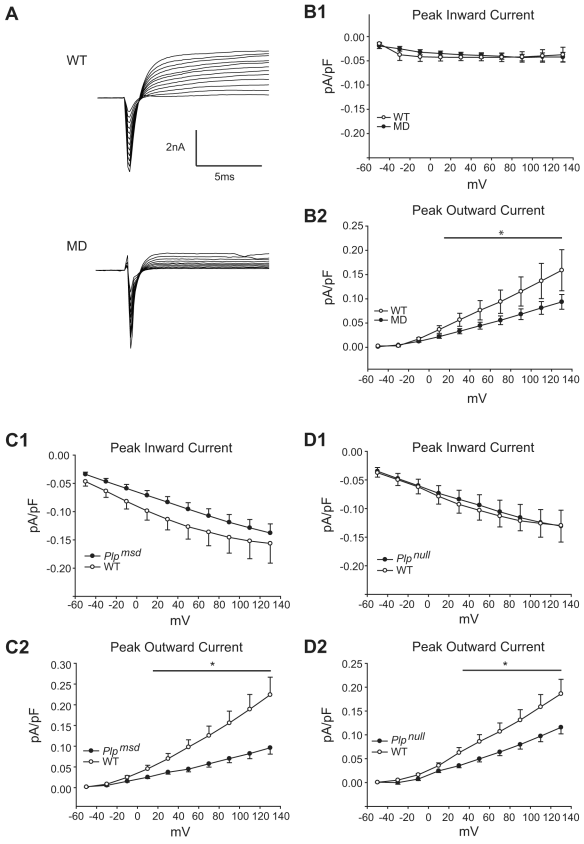

Figure 2.

Current-voltage relationships in *Plp* mutant animals differ from wild type littermates. A: Representative raw traces of current evoked in a WT nTS cell at P21 (upper panel) and in an nTS cell from an MD rat (lower panel) during the stimulus protocol. B: Current voltage relationships at P21 in commissural nTS neurons from both WT control and MD rats. B1: There was no difference between WT control and MD nTs cells in the peak inward current Neurons from MD rats at P21. B2: (closed circles) showed decreased outward currents at voltage steps above 10 mV when compared to nTS cells from WT control rats (B2, open circles) (n=16 for control cells and n=25 for MD cells). C1: Peak current was normal in Plp^{msd} mice when compared to WT controls. C2: Outward current was significantly reduced in Plp^{msd} mice at voltage steps above 10mV when compared to WT littermate controls (n=11 for Plp^{msd} and n=20 for Plp^{msd} control). D1: Peak current was normal in Plp^{null} mice when compared to WT controls. D2: Outward current was significantly reduced in Plp^{null} mice at voltage steps above 10mV when compared to WT littermate controls (n=16 for both Plp^{null} and control) * indicates $p < 0.01$. pA, picoamperes; pF, picofarads; mV, millivolts. nA, nanoamperes; ms, milliseconds.

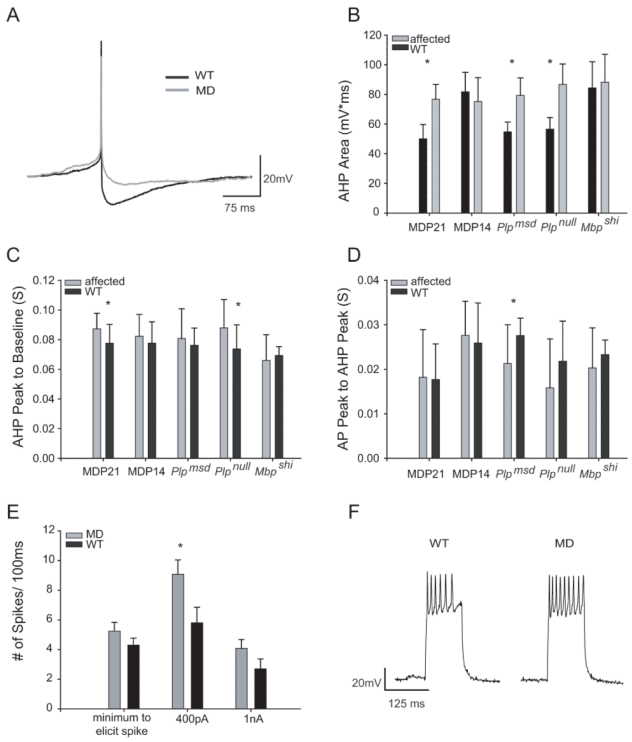

Figure 3.

Comparison of action potentials in MD rats and *Mbp*^{shi}, *Plp*^{msd}, and *Plp*^{null}, mice. A: Comparison of the action potential from a P21 MD rat (grey trace) and a WT littermate control (black trace) shows a deficit in afterhyperpolarization (AHP) in MD rats. Each trace is the average of 10 spikes per cell. B: The area of the AHP is significantly reduced in cells from P20–24 MD, *Plp*^{msd}, and *Plp*^{null} mice. C: The time from the peak of the AHP to the return to baseline is significantly longer in P21 MD and *Plp*^{null} mice when compared to WT controls. D: The time from the peak of the action potential to the peak of the AHP is significantly shorter in *Plp*^{msd} mice when compared to WT controls. E: Histogram comparing the number of spikes fired in response to current input. NTS neurons from MD rats and P20–24 fire significantly more spikes in response to 400pA stimulation when compared to cells from WT controls. F: Representative current clamp traces from nTs neurons from MD and WT rats at P21 in response to 400nA stimulation. * indicates $p < 0.05$. mV, millivolts; ms milliseconds, S, seconds.

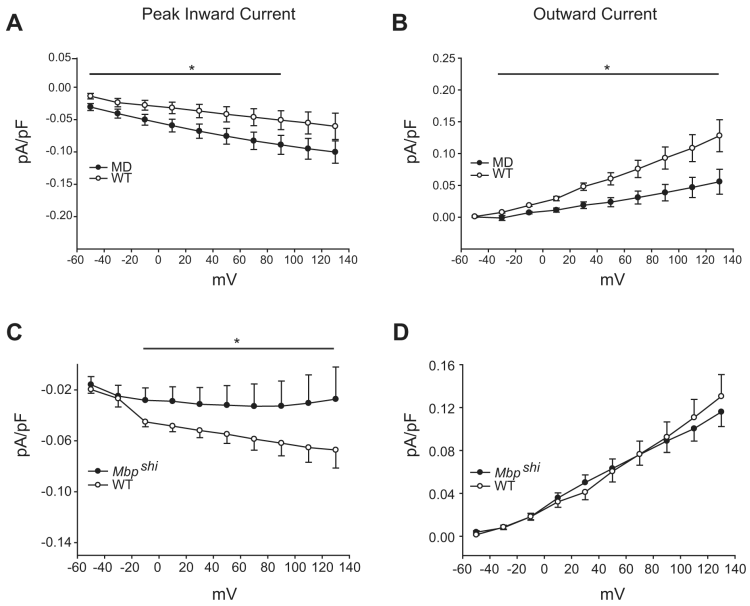

Figure 4.

A: In the VLM neurons from P21 MD rats showed significantly increased peak inward currents at voltage steps from −50 to +90mV when compared to Wt controls. B: VLM cells also showed decreased outward current at voltages from −30 to +130 when compared to WT controls. (n=11 for MD and n=10 for control.) C: Peak inward current was significantly reduced in nTS cells from P21 *Mbp*^{shi} mice when compared to cells from WT control mice. D: However, outward current in *Mbp*^{shi} nTS cells was not significantly different from WT nTS cells (n=16 for both *Plp*^{null} and control).

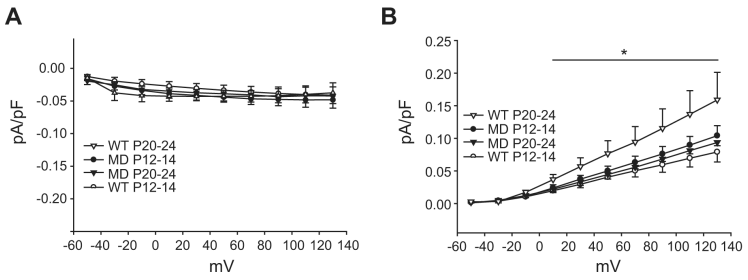

Figure 5.

Developmental maturation of outward current failed to occur in MD rats between P12–14 and P20–24. A: No significant difference in peak inward current was seen between MD and WT nTS cells at P12–14 or P20–24. B: At P12–14 outward current was not significantly different between MD and WT nTS cells(n=14 for WT cells, n=22 for MD cells). However, at P20–24 there was a significant difference in outward current between nTs cells from MD and WT rats (triangles; n=16 for WT control cells, n=22 for MD cells). * indicates $p < 0.05$. pA, picoamperes; pF, picofarads; mV, millivolts.

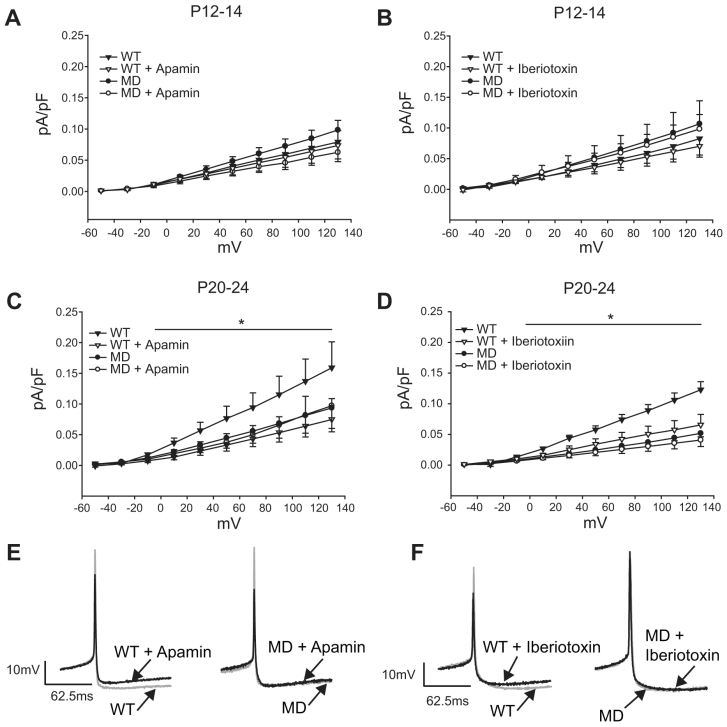

Figure 6.

NTS neurons from MD rats lack functional BK and SK channels at P21. A&B: At P12–14, neither blockade by apamin (SK cahnnels) nor iberiotoxin (BK channels) had a significant effect on outward current in MD or WT control nTS cells (apamin: control n=8, MD n=9; iberiotoxin: n=9, both groups). C&D: At P20–24, both apamin and iberiotoxin significantly inhibited outward currents in nTS cells from WT control, but not MD rats. This indicates a lack of functional SK and BK channels in these cells (apamin: n=8 both groups; iberiotoxin: n=9, both groups). * indicates $p < 0.05$ for apamin, and $p < 0.04$ for iberiotoxin at voltage steps above −10 mV. E&F: Current clamp recordings of action potentials from a P21 MD (black traces) and WT control (grey traces) nTS cells reveal that apamin and iberiotoxin significantly decrease the AHP in nTS cells from WT control rats while apamin and iberiotoxin have no effect on action potentials in nTS cells from MD rats (apamin: n=8 both groups; iberiotoxin: n=9, both groups). pA, picoamperes; pF, picofarads; mV, millivolts; ms, milliseconds.

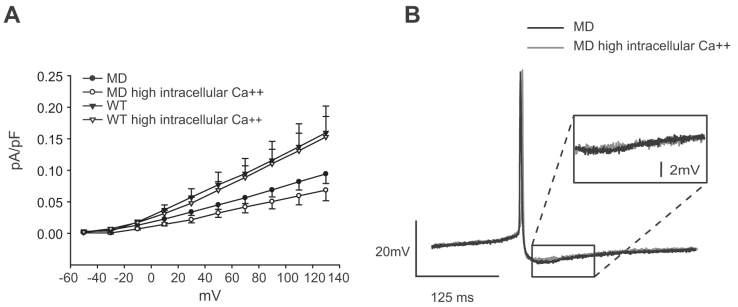

Figure 7.

High (buffered) intracellular calcium failed to correct the deficit in outward current in nTS cells from P21 MD rats. A: Outward current in nTS cells from MD (circles; n= 25 MD, n=11 MD high intracellular calcium) and WT control rats (triangles; n=16 control, n=14 control high intracellular calcium) is not significantly changed in the presence of high buffered intracellular calcium (400nM free calcium). B: Action potentials recorded in current clamp from an MD nTS cell in the presence of normal intracellular calcium (black trace) and in high buffered intracellular and low extracellular calcium (grey trace) also reveal no significant changes in APs between these two conditions indicating that the deficits seen in MD nTS cells are likely not secondary to effects from altered calcium dynamics in these cells. pA, picoamperes; pF, picofarads; mV, millivolts.

Table 1

Cellular properties of nTS neurons

Animal	V_m	C_m	R_m
P14 MD	−42.5 ± 1.7 mV	33.6 ± 3.9 pF	784 ± 73 MΩ
P14 WT	−50.1 ± 2.5 mV*	33.5 ± 2.9 pF	740 ± 130 MΩ
P21 MD	−44.2 ± 1.3 mV	37.7 ± 2.2 pF	719 ± 58 MΩ
P21 WT	−41.4 ± 1.8 mV	31.9 ± 3.0 pF	730 ± 71 MΩ
Mbp^{shi}	−50.0 ± 1.6 mV	23.5 ± 2.6 pF	714 ± 104 MΩ
Mbp^{shi} control	−40.3 ± 2.9 mV*	25.6 ± 2.0 pF	885 ± 41 MΩ
plp^{msd}	−53.0 ± 3.7 mV	15.5 ± 1.6 pF	720 ± 178 MΩ
plp^{msd} control	−47.2 ± 2.0 mV	18.4 ± 2.1 pF	789 ± 66 MΩ
plp^{null}	−43.6 ± 4.1 mV	24.7 ± 2.7 pF	855 ± 107 MΩ
plp^{null} control	−41.5 ± 3.3 mV	27.0 ± 3.6 pF	863 ± 148 MΩ

Values are means ± s.e.m., n=11–26/group.

* $p < 0.05$. V_m = resting membrane potential, C_m = capacitance, R_m = membrane resistance.